TAO, Vol. 9, No. 3, 329-344, September 1998

Imaging of Arc-Arc Collision in the Ryukyu Forearc Region Offshore Hualien From TAICRUST OBS Line 16

Tan K. Wang[1] and Chun-Hsien Chiang[1]

(Manuscript received 7 January 1998, in final form 27 August 1998)

ABSTRACT

A velocity-depth model, developed using the travel-time inversion of data from Ocean Bottom Seismometers on TAICRUST OBS Line 16, in the western Ryukyu forearc region is described in this paper. Phase identifications of refracted and reflected signals, initial model building from the shallow to the deep structures, and comparison with a synthetic seismogram have been used to reduce the non-uniqueness of the velocity model.

The velocity contours of the model indicate, from west to east, (1) a thick forearc sedimentary layer below the Hsincheng Ridge, (2) a wedge-shaped upper crust with high velocity gradients beneath the Hoping Basin, and (3) a depression within the western Ryukyu Arc below the Nanao Basin. The thickness of the forearc sediment (3 - 4.5 km/sec) beneath the Hsincheng Ridge is found to be about 10 km in the model. Based on the similarity of P-wave velocities for the Luzon Arc, the Coastal Range and the Yaeyama accretionary wedge, the forearc sediment may result from the arc-continent collision and/or the bending of the western Ryukyu Arc. The upper and the lower boundaries of the upper crust (mainly the Ryukyu Arc) are better defined by two velocity contours of 4.5 km/sec and 6.25 km/sec according to the contrast of the velocity gradient in the model. The high velocity gradient with the west-dipping velocity contours beneath the Hoping Basin and a depression about 5 km deep below the western half of the Nanao Basin are thus found in the upper crust. We infer that the high velocity gradient and the depression in the upper crust may be generated by the collision of the northern Luzon Arc and the western Ryukyu Arc.

Both basement (forearc sediment and Ryukyu Arc basement) deepening and crustal thickening westward in this study are similar to those in velocity models from TAICRUST OBS Line 14 and the onshore-offshore line across central Taiwan. The tectonic motions of the northern Luzon Arc, the western Ryukyu Arc and the subducting slab of the Philippine Sea Plate interpreted in this paper provide possible mechanisms for the induction of high seismicity in the western Ryukyu forearc region.

[1]Institute of Applied Geophysics, National Taiwan Ocean University, Keelung 20224, Taiwan, ROC

(Key words: OBS, Travel-time inversion, Forearc sediment, Arc-arc collision, Luzon Arc, Ryukyu forearc, Philippine Sea Plate)

1. INTRODUCTION

The active plate motions in Taiwan have evolved from subduction, arc-continent collision, arc-accretion and arc-arc collision since 6.5 Ma (Huang *et al.*, 1998). Most of these tectonic systems can currently be observed in the western Ryukyu forearc region and involve the subduction of the Philippine Sea Plate (PSP) (Wang *et al.*, 1996), similarity in P-velocity of the northern Luzon Arc and Yaeyama accretionary wedge (Cheng *et al.*, 1996), and the former collision of the Luzon Arc and the Ryukyu Arc (Hsu and Sibuet, 1995). The interactions of these systems are both complex and active, and induce high seismicity offshore Hualien. The focal mechanisms in Figure 1 further indicate the dominance of the thrust faulting (red) and lateral compression (blue) in the Ryukyu forearc region (Kao *et al.*, 1998).

By analyzing the bathymetric data, a shear zone was found in a junction area covering the northern Luzon Arc, the PSP and the western Ryukyu Arc (Lallemand *et al.*, 1998). The shear force south of the Hoping Basin drives the northwestward movement of the accretionary wedge toward the Hsincheng Ridge. Cheng *et al.* (1996) confirmed the northeastward extension of the northern Luzon Arc both below the Hsincheng Ridge and to the accretionary wedge using onshore and offshore seismic data. However, neither the deformation of the PSP and the northern Luzon Arc, nor the collision of the northern Luzon Arc and the western Ryukyu Arc have been identified. East of the junction, a tear fault boundary (Lallemand *et al.*, 1997) and a subducting asperity (Wang *et al.*, 1996) below the Nanao Basin were proposed. However, these structural boundaries (e.g. velocity interfaces) below the Nanao Basin and the driving forces could still not be specifically determined. Further eastward, it was inferred that the Gagua Ridge subducted between the Nanao Basin and the East Nanao Basin (Schnurle *et al.*, 1998). The subduction of the Gagua Ridge may thus be one of the tectonic motions that affect the crustal structure below the Nanao Basin.

The aims of this paper are to address the above unsolved issues that include the deformation of the PSP, the northern Luzon Arc and the western Ryukyu Arc, the possibility of arc-arc collision, the structural boundary between the overlying western Ryukyu Arc and the subducting PSP, and their associated driving mechanisms. We believe that clarification of the tectonic motions in the western Ryukyu forearc region can provide new insights into the high seismicity offshore Hualien.

The best strategy for achieving the above goals is to implement a combined Ocean Bottom Seismometer (OBS) and Multi-Channel Seismic (MCS) survey because it can generate the velocity-depth models with the high resolution for both the shallow and crustal structures (Holbrook *et al.*, 1994). An OBS survey offshore eastern Taiwan was first conducted by Hagen *et al.* (1988). Their results illustrated the northward subduction of the PSP beneath the western Ryukyu Arc (Hagen *et al.*, 1988; Wang and Chen, 1988). However, using explosives as seismic sources and without a combined MCS survey, the first OBS survey could not provide a detailed velocity model in the western Ryukyu forearc region.

In the summer of 1995, a deep seismic survey offshore Taiwan (known as TAICRUST)

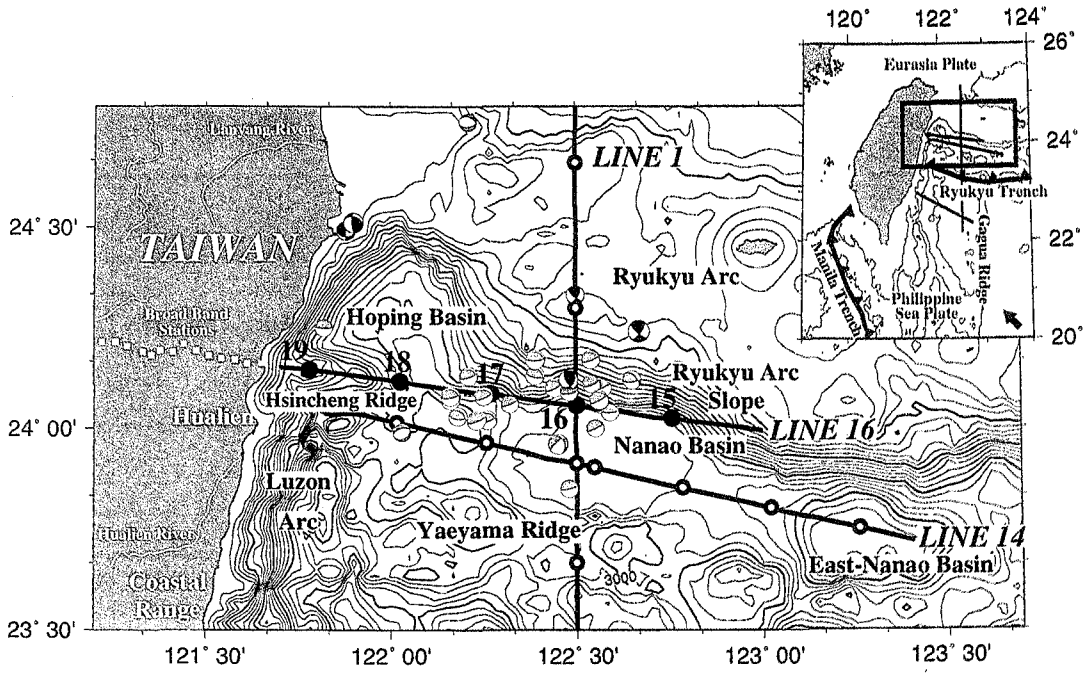

Fig. 1. OBS seismic lines in the western Ryukyu forearc region offshore Hualien. Black and white circles indicate OBS stations along Line 16 and other lines. White squares denote land stations across central Taiwan (Shih *et al.*, 1998). Velocity model of OBS Line 16, spanning the Hsincheng Ridge, the Hoping Basin, the northern edge of the Nanao Basin and the Ryukyu Arc Slope, is investigated. Contour interval of the bathymetric data (Hsu *et al.*, 1996) is 200 m. Focal mechanisms in red, blue and purple for compressional quadrants denote under-thrusting of the PSP, lateral compression in the Ryukyu Arc and normal faulting, respectively (Kao *et al.*, 1998). Depths of focal mechanisms are less than 40 km (see Figure 7(a)).

was carried out using a large air-gun array (20 guns) and a long streamer from the R/V Maurice Ewing, and by deploying OBSs from the R/V Ocean Researcher I (Liu *et al.*, 1995). High-quality MCS data were produced to image the deep structures offshore Taiwan (Liu *et al.*, 1995; Liu *et al.*, 1997). In addition, four-component (hydrophone, vertical and two horizontal channels) OBS data were collected and processed to generate the velocity-depth models of the crustal structures offshore eastern Taiwan (Wang *et al.*, 1996; Chiang, 1997; Wang, 1997; McIntosh and Nakamura, 1998; Yang and Wang, 1998).

In this paper, a P-wave velocity model in the Ryukyu forearc region offshore Hualien, as illustrated by OBS Line 16 in Figure 1, is investigated. Five OBS instruments, denoted by

black circles in Figure 1, were deployed from west to east spanning the Hsincheng Ridge, the Hoping Basin, the northern edge of the Nanao Basin and the southern flank of the Ryukyu Arc Slope. The Luzon Arc and the Coastal Range are to the southwest of OBS Line 16 while the Ryukyu Arc is located to the north. Other OBS lines, Lines 1 (Wang *et al.*, 1996) and 14 (McIntosh and Nakamura, 1998) denoted by connecting white circles in Figure 1, in the western Ryukyu forearc region and the onshore-offshore line (white squares in Figure 1) across central Taiwan (Shih *et al.*, 1998) can also provide constraints for the tectonic structures in this area.

2. PHASE IDENTIFICATION AND TRAVEL-TIME INVERSION OF OBS DATA

The steps required to generate the crustal velocity model include pre-processing and phase identification of the OBS data, initial model building, ray tracing of the selected arrivals, and travel-time inversion. The various procedures are described below.

2.1 Pre-processing of the OBS Data and Identification of the Arrivals

OBS raw data were processed through station relocation (Christeson, 1995), band-pass filtering and trace balancing (Henkart, 1998) before display. Figures 2 - 4 illustrate the vertical component of OBS data for stations 15 - 17, respectively. In the following, a reduced velocity of 8 km/sec is applied for all travel-time axes as the reduced time in Figures 2-4, 5(d) and (6).

OBS data from station 15 (on the Ryukyu Arc Slope) in Figure 2 show earlier arrivals on the east side that imply a shallower sea-floor and/or higher apparent velocities east of the station. Phase identification of OBS data is generally on a trial-and-error basis. However, in the vertical component of OBS data for Line 16 (see Figures 2-4), all first arrivals are identified as refractions while the later arrivals correspond to reflections. As the offset increases, the refracted and reflected signals are through deeper structures. For example, the refracted arrivals, which traveled through the sediment (Ps), the crust (Pg) and returned from the upper mantle (Pn) in Figure 2, are the first arrivals with increasing offsets. A reflection from the Moho (PmP) is also observed as a later arrival between the offsets at 45 km and 75 km west of the station in Figure 2.

Refractions through the crust (Pg) in Figure 3 are faster and weaker east of station 16 (on the northern edge of the Nanao Basin) that result from the bathymetric effect of the Ryukyu Arc Slope and the low transmission of energy for rays below the Ryukyu Arc Slope. Reflections from the bottom of the sedimentary layer (PsP) and from the Moho (PmP) are also found in Figure 3 and can provide more depth constraints for these interfaces. Clear inter-crustal reflections (PcP) are shown in OBS data from station 17 in Figure 4. Similarly with Figures 2 and 3, the refracted signals from east of the station are faster so that the general trend of the west-dipping velocity contours (including the sea-floor) can be inferred.

We have picked more than 3000 travel times from the five OBS stations. The uncertainty of these picks is generally less than 0.02 sec except for the far-offset and the later arrivals. The velocity model will probably be more reliable if we can identify other later arrivals with good signal-to-noise ratio.

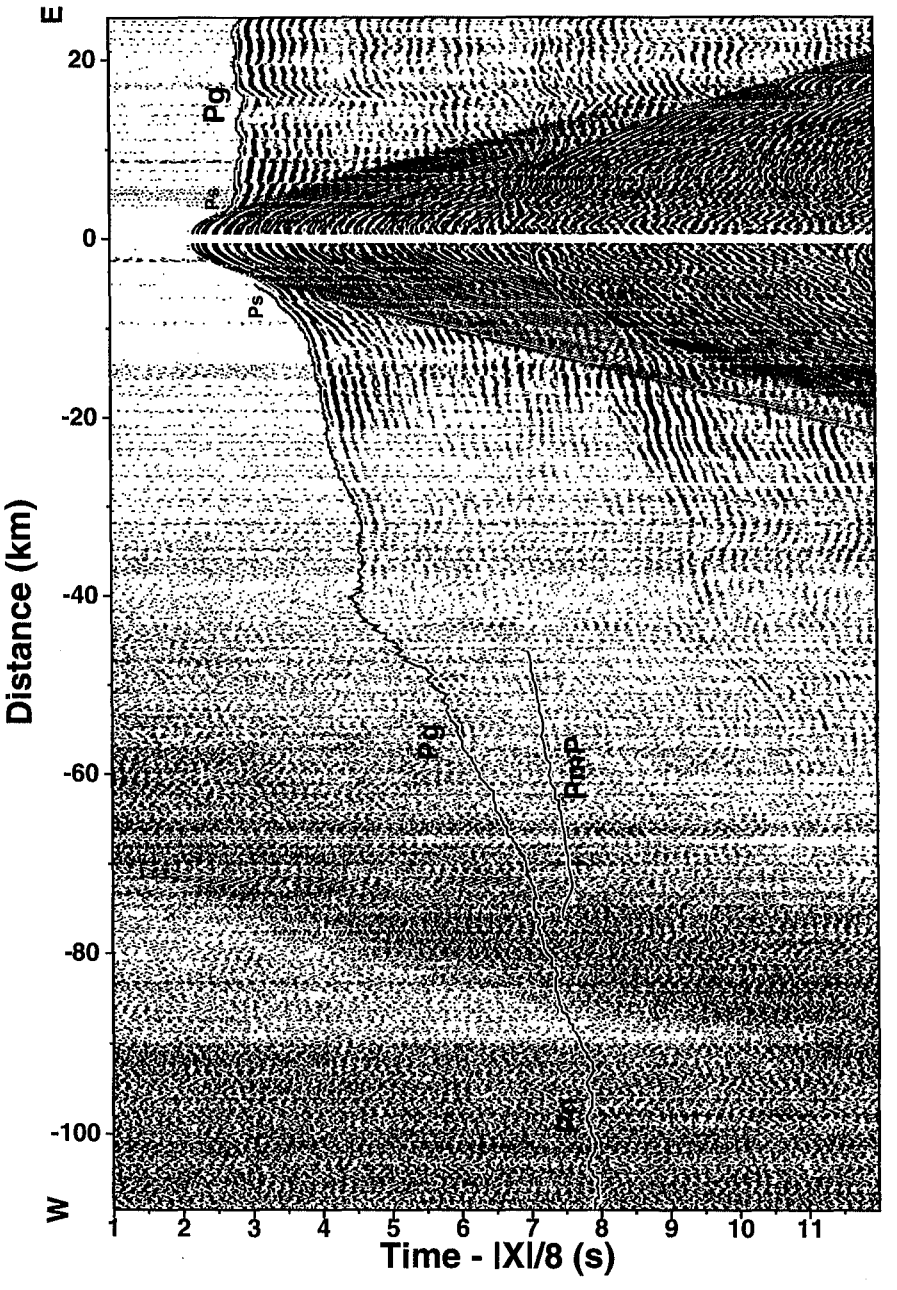

Fig. 2. Vertical component of OBS data and picked arrivals (solid lines) for station 15. Reduced velocity of 8 km/sec is applied. The station is located on the Ryukyu Arc Slope. Refracted signal through the mantle, Pn, is identified for offset beyond 90 km. Reflections from the Moho, PmP, can also be seen between offsets of 48 km and 78 km.

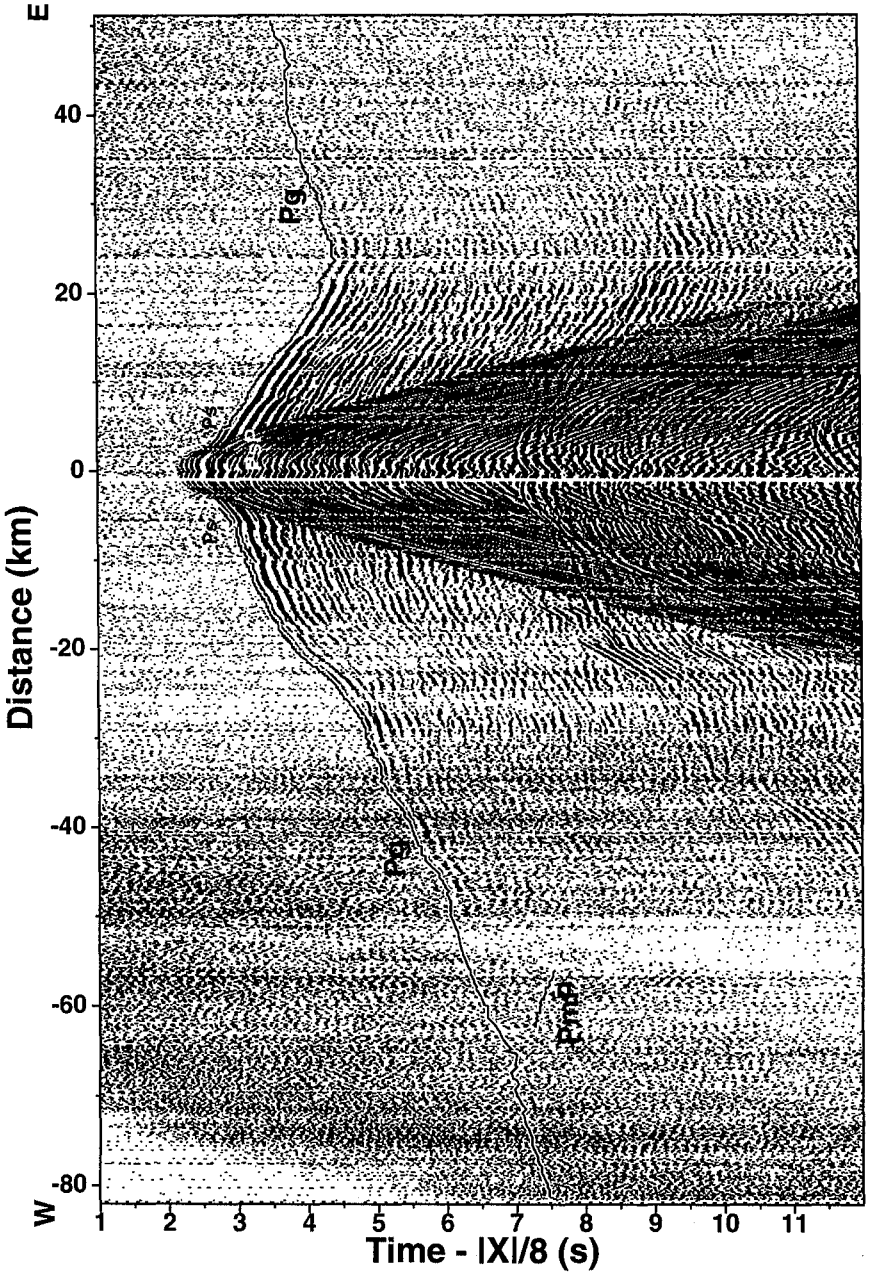

Fig. 3. Vertical component of OBS data and picked arrivals (solid lines) for station 16. This station is located on northern edge of the Nanao Basin. Refraction through the crust, Pg, east of the station is faster than that to the west that may result from the eastward shallow sea-floor and/or the high apparent velocity of the crust east of the station.

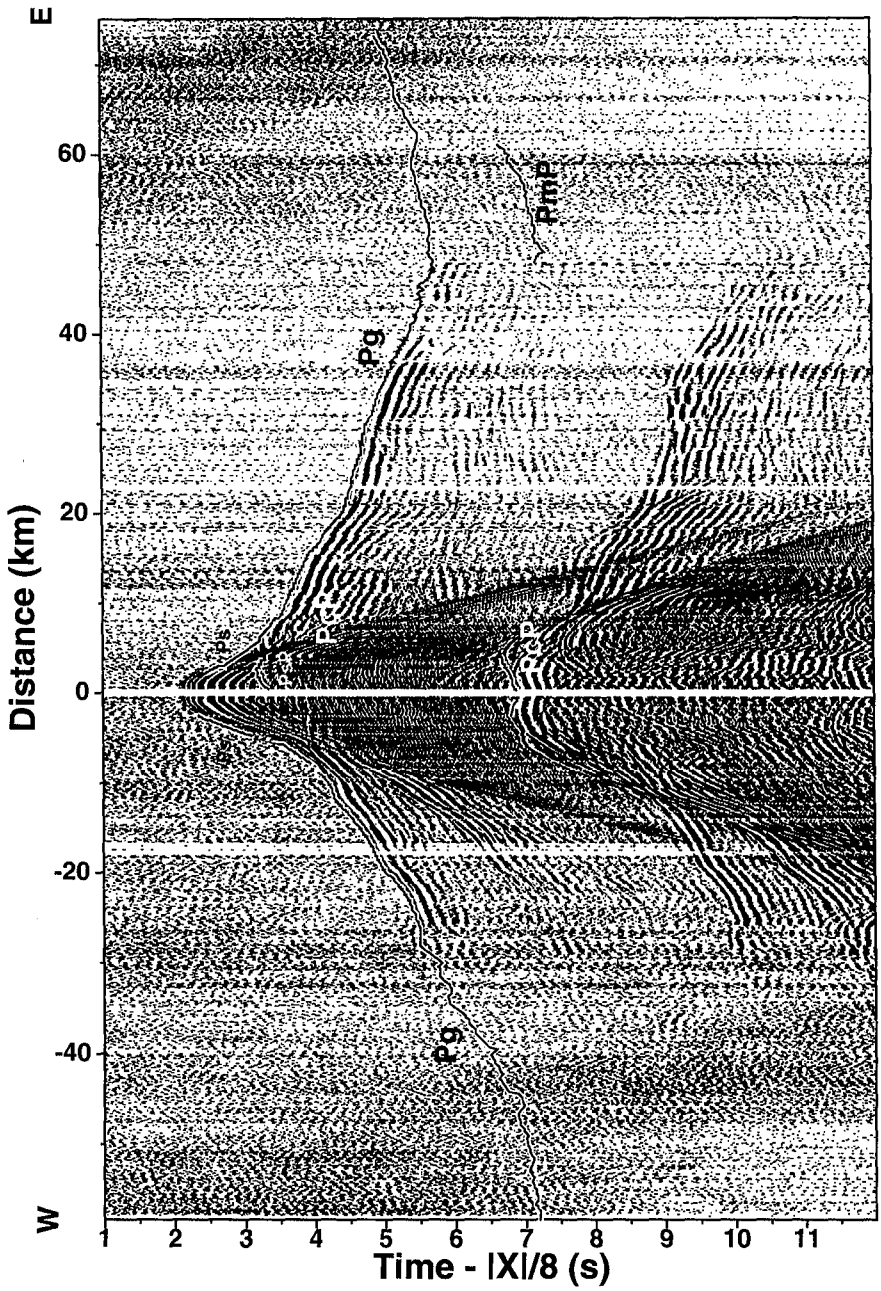

Fig. 4. Vertical component of OBS data and picked arrivals (solid lines) for station 17. Reflections from the bottom of the sedimentary layer, PsP, and from the interface in the crust, PcP, are picked from the near-offset (< 10 km) of OBS data.

2.2 Ray Tracing and Travel-time Inversion

We successively constructed the velocity model from the shallow to the deep layers. The shallow model must be well constrained before working on the next deeper layer. Figures 5(a)-(c) demonstrate the ray coverage and how good the constraints are from the shallow to the deep layers, respectively. The rays in green indicate the refractions while the reflections are denoted by other colors. Refracted rays in Figures 5(a)-(c) provide good velocity constraints for the sedimentary and crustal structures in the model. The geometry of the sedimentary layers, some inter-crustal interfaces and the Moho are better determined from reflections as shown in Figures 5(a) and (c). Two travel-time inversions, the damped least-squared (Zelt and Smith, 1992) and the conjugate gradient (Operto, 1995) methods, were applied in turn to develop our velocity model. The former method can provide small but delicate adjustments to the model while the latter can handle the dense grids of the model but without solving the corresponding matrix. Figure 5(d) displays the calculated (color) and the picked (black dots) travel times for OBS Line 16. Travel times fit fairly well and the total RMS error of 0.146 sec proves the accuracy of the velocity model.

2.3 Comparison With the Synthetic Seismogram

A synthetic seismogram from OBS station 15 is displayed in Figure 6 by applying the similar gain with the associated OBS data in Figure 2. The amplitudes of the refracted arrivals through the upper mantle (Pn) and the reflected arrivals from the Moho (PmP) in the seismogram are strong. The comparison of the OBS data in Figure 2 and the synthetic seismogram in Figure 6 shows the consistencies of the travel times and the amplitudes that again support the velocity model.

Non-uniqueness of the P-wave velocity model can be further reduced by comparing with other synthetic seismograms, the gravity model and the shear wave velocity model. Most of these comparisons have been conducted by Wang *et al.* (1998).

3. IMPACTS OF LUZON ARC, RYUKYU ARC AND PSP IN THE RYUKYU FOREARC REGION

The P-wave velocity model in Figure 7(a) spans the Hsincheng Ridge, the Hoping Basin, the northern edge of the Nanao Basin and the Ryukyu Arc Slope in the western Ryukyu forearc region. The interval of the velocity contour in Figure 7(a) is set at 0.25 km/sec. In order to realize the boundaries of various tectonic provinces and their interactions, five velocity contours of 1.51, 3, 4.5, 6.25 and 7.8 km/sec are chosen according to the velocity contrasts and the velocity gradients in Figure 7(a). In the following, we shall describe and interpret our velocity-depth model in terms of these velocity boundaries and associated tectonic structures.

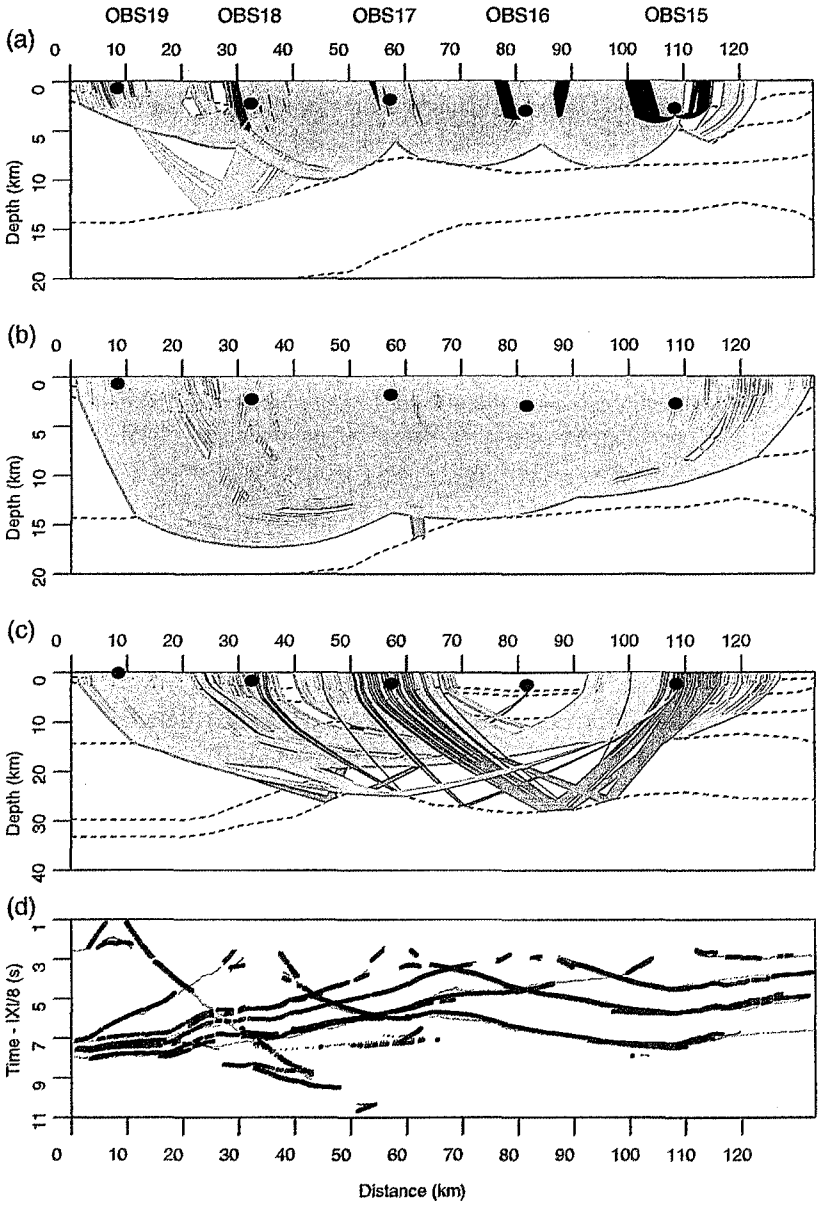

Fig. 5. Travel-time inversion of the P-wave velocity model along OBS Line 16. (a) Refracted (dark blue and green) and reflected (orange and pink) rays through the sediment and the compacted sediment, (b) refracted (green) and reflected (light blue) rays through the upper crust, (c) refracted (green) and reflected (red) rays through the lower crust, (d) calculated (color) and picked (black dot) travel times for five OBS stations.

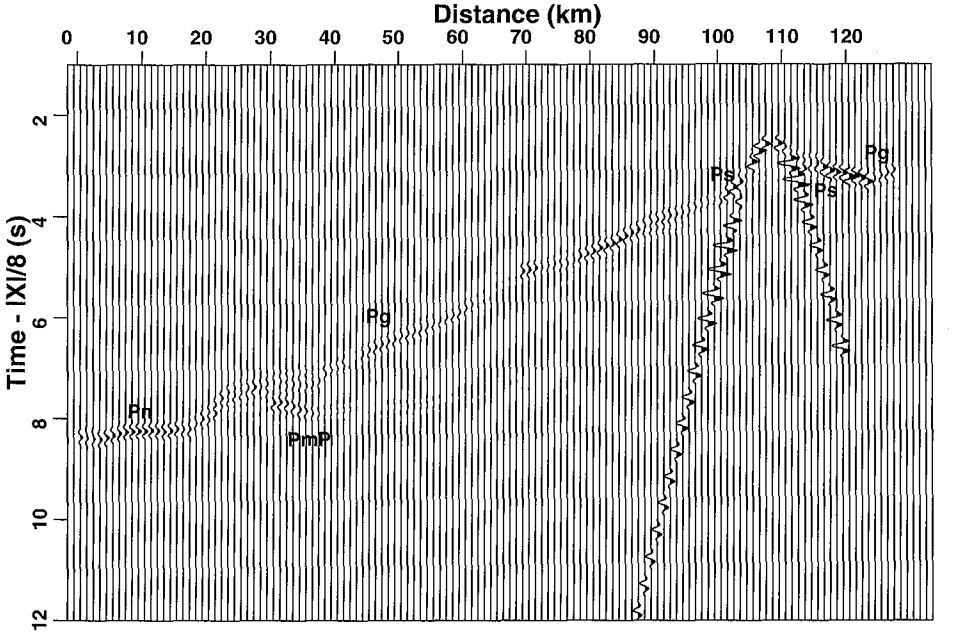

Fig. 6. Synthetic seismogram of the vertical component from OBS station 15. Strong amplitudes of the far-offset and later arrivals (Pn and PmP) are consistent with observation from OBS data in Figure 2.

3.1 Sediment (P-wave velocity = 1.51 - 3 km/sec)

As shown in Figure 7(a), thickness and P-wave velocity of the sediment below the Hsincheng Ridge are, respectively, about 2 km and less than 2.3 km/sec while those in the Hoping Basin are 3 - 4 km and higher than 2.3 km/sec, respectively. This implies that the sediment below the Hsincheng Ridge is younger, but that the Hoping Basin provides a better environment for sediment accumulation. The lower sediment in the Hoping Basin has been indicated as an old Suao Basin (Lallemand *et al.*, 1997), and this is consistent with our interpretation. In view of the bathymetry (Hsu *et al.*, 1996) in Figure 1, the main sources of these sediments are the Taiwan mountain-belt via Lanyang River and Hualien River which are, respectively, to the northwest and southwest of OBS Line 16. In contrast, no sediment is seen in the eastern portion of the velocity model because that portion of the OBS Line 16 lies along the northern edge of the Nanao Basin and the steep topography of the Ryukyu Arc Slope.

3.2 Compacted Sediment (P-wave velocity = 3 - 4.5 km/sec)

We interpret the layer with P-wave velocity of 3 - 4.5 km/sec as compacted sediment. In our velocity model (see Figure 7(a)), an anomalously thick compacted sediment about 10 km

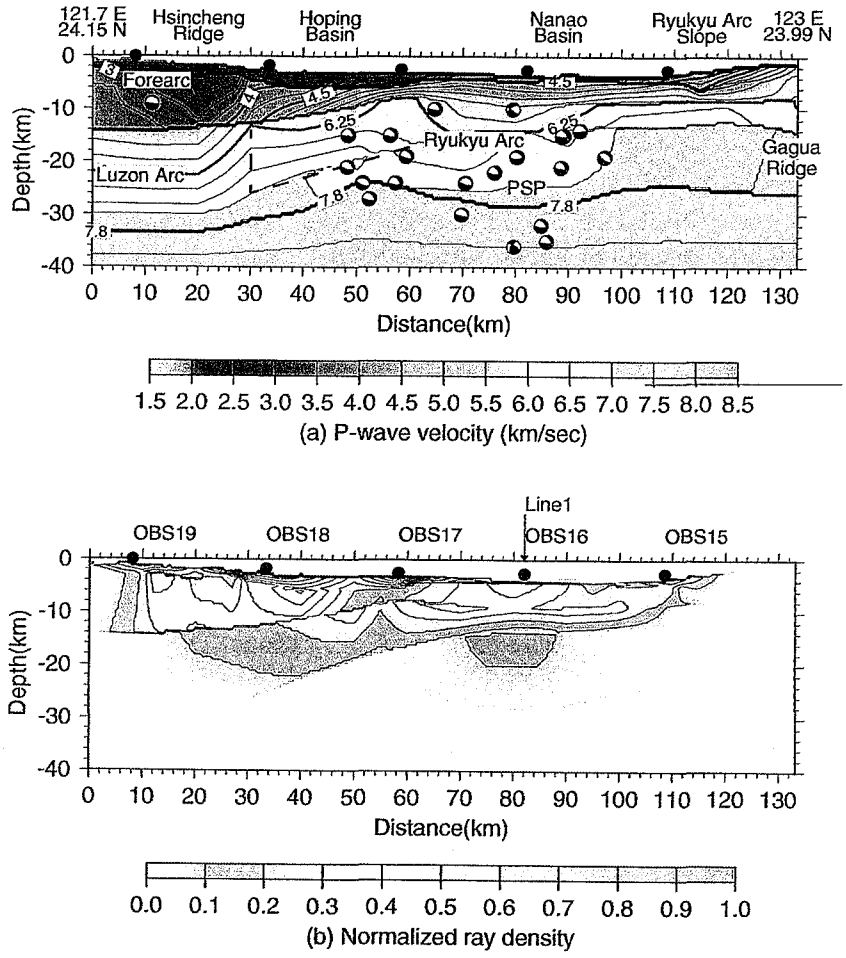

Fig. 7. (a) Velocity model of the P-wave along OBS Line 16 as shown in Figure 1. Interval of the velocity contour is 0.25 km/sec. OBS stations are denoted by black circles. Thick forearc sediment, bounded by the velocity contours of 3 and 4.5 km/sec, is displayed below the Hsincheng Ridge. Crustal structures of the velocity model consist of the Ryukyu Arc basement below the Nanao Basin, the northern Luzon Arc at the west end, the PSP beneath the Ryukyu Arc basement and the Gagua Ridge at the east end. Vertical and inclined dashed lines beneath the Hoping Basin may indicate the eastern edge of the northern Luzon Arc and the top of the western PSP. Cross sections of focal mechanisms in Figure 1 within 10' of OBS Line 16 are projected onto the velocity model. Error of the focal depth is about 5 km. (b) Normalized ray density of the travel-time modeling. Ray density is generally high (> 0.5) for the model at less than 15 km depth.

thick with v-shaped velocity contours is found below the Hsincheng Ridge. The thickness of the compacted sediment then decreases eastward from about 8 km thick below the eastern toe of the Hsincheng Ridge to less than 0.5 km thick below the Hoping Basin. The P-wave velocity of this wedge-shaped compacted sediment (> 4 km/sec) is higher than that below the Hsincheng Ridge (< 4 km/sec). Since the P-wave velocity of the thick forearc sequences in Figure 7(a) is similar to those obtained in the Coastal Range (Tsai *et al.*, 1974) and in the Yaeyama accretionary wedge (Cheng *et al.*, 1996), we infer that the forearc sediment below the Hsincheng Ridge resulted from the collision of the northern Luzon Arc and the Eurasian Continent (Huang *et al.*, 1998) and/or from the bending of the western Ryukyu Arc (McIntosh and Nakamura,1998). The compression from the collision also pushed the Hsincheng Ridge eastward, resulting in both the nearly vertical velocity contour of 4 km/sec below the eastern toe of the Hsincheng Ridge and the higher velocity of the wedge-shaped compacted sediment.

Below the Nanao Basin, the compacted sediment is about 1 km thick, but this suddenly increases to 3 km and then gradually decreases eastward below the Ryukyu Arc Slope. Schnurle *et al.* (1998) suggested that the Gagua Ridge subducts northward between the Nanao Basin and the East Nanao Basin. If the Gagua Ridge extends further northward beneath the Ryukyu Arc Slope, it may appear at the east end of the model as shown in Figure 7(a). Therefore, we interpret the decreasing thickness of the compacted sediment below the Ryukyu Arc Slope to be the result of the northward subduction of the Gagua Ridge. The source of the compacted sediment, with a P-wave velocity higher than 4 km/sec, below the Ryukyu Arc Slope is still unknown.

3.3 Crust (P-wave velocity = 4.5 - 7.8 km/sec)

The crustal thickness along OBS Line 16 in Figure 7(a) remains almost uniform between 20 - 25 km. A velocity contour of 6.25 km/sec is chosen as the boundary between the upper crust and the lower crust in the eastern portion of the model because the velocity gradient above the boundary is much higher than that below it as illustrated in Figure 7(a). A wedge-shaped upper crust with the west-dipping velocity contours and the high velocity gradient can be seen beneath the Hoping Basin. Further eastward below the western half of the Nanao Basin, a depression about 5 km deep in the upper crust is found. The widths of the depression at the top and bottom are 35 km and 18 km, respectively. Since OBS stations 15 - 17 were located on the Ryukyu Arc Slope (Figure 1), the upper crust east of the Hoping Basin should be the Ryukyu Arc basement as indicated in Figure 7(a).

Tectonic structures of the lower crust are more complex and less constrained in the velocity model. Cheng *et al.* (1996), Huang *et al.* (1998) and Lallemand *et al.* (1998) supported the northward extension of the Luzon Arc as the role of the oceanic crust below the Hsincheng Ridge. By considering the velocity models of OBS Line 16 (see Figure 7(a)), Line 14 (McIntosh and Nakamura,1998) and the onshore-offshore line across central Taiwan (Shih *et al.*, 1998), the northern Luzon Arc extends below the Hsincheng Ridge with a crustal thickness of about 20 km while the top of the northern Luzon Arc is about 14 km and 9 km below sea level along OBS Lines 16 and 14, respectively. Similarly, the velocity model from OBS data off-

applied to optimize the grids of the model. The normalized ray density is greater than about 0.5 for most of the velocity model shallower than 15 km (Figure 7(b)). For the velocity model between 15 km and 20 km in depth, the normalized ray density is about 0.2. Therefore, the sediment, the compacted sediment and the upper crust in Figure 7(a) are more reliable in this study.

4. CONCLUSIONS

In this paper, the forearc sediment below the Hsincheng Ridge, the collision of the northern Luzon Arc and the western Ryukyu Arc, the western boundary of the PSP beneath the Hoping Basin and the oblique subduction of the PSP beneath the western Ryukyu Arc offshore Hualien are imaged and interpreted from an OBS model of Figure 7(a). The general trend of the forearc sediment and the crustal structures in this study (*i.e.* both basement deepening and crustal thickening westward) are similar to velocity models from TAICRUST OBS Line 14 (McIntosh and Nakamura, 1998) and the onshore-offshore line across central Taiwan (Shih *et al.*, 1998).

If we believe that the Luzon Arc is currently below the forearc sediment and near the coast, as suggested by Cheng *et al.* (1996), Huang *et al.* (1998) and Lallemand *et al.* (1998), then the forearc sediment below the Hsincheng Ridge, which is 10 km thick between the northern Luzon Arc and the sediment along OBS Line 16, may result from the former forearc basins of the Coastal Range (Huang *et al.*, 1998) and/or the Yaeyama accretionary wedge (Schnurle *et al.*, 1998; McIntosh and Nakamura, 1998). Other OBS velocity models, Line 14 (McIntosh and Nakamura, 1998) and Line 23 (Yang and Wang, 1998), also show the thick forearc sediment near the coast. Furthermore, the top of the Luzon Arc in the velocity models of this paper, OBS Line 14 and OBS Line 23 are 14 km, 9 km and 5 km below the sea level, respectively, although these portions of the velocity models are less constrained and subject to the incorporation of onshore-offshore seismic data (Shih *et al.*, 1998; Yeh *et al.*, 1998). The rapid vertical offset of the top of the northern Luzon Arc from OBS Line 14 to Line 16 favors the proposed tear fault (Lallemand *et al.*, 1997) between these two lines.

The boundaries of the upper crust (mainly the Ryukyu Arc basement) may be defined by two velocity contours of 4.5 km/sec and 6.25 km/sec according to the velocity contrast and the velocity gradient in Figure 7(a). In this paper, a wedge-shaped upper crust with high velocity gradients beneath the Hoping Basin and a depression about 5 km deep in the upper crust below the western half of the Nanao Basin can be seen as evidence for the arc-arc collision. In addition, by considering the velocity contours and the focal mechanisms, the boundary of the PSP and the arc (Luzon and/or Ryukyu) below the Hoping Basin is westward dipping from 16 km to 26 km in depth.

In this paper, the boundaries of the northern Luzon Arc, the western Ryukyu Arc and the Gagua Ridge cannot be determined specifically. P-wave velocity models (Wang *et al.*, 1996) and shear wave velocity models (Wang, 1997) of other OBS Lines as shown in Figure 1 may enhance or update the clarity of these boundaries, and may provide many more new insights into the arc-arc collision offshore Hualien. Furthermore, the combination of the velocity models from the OBS data and from the onshore-offshore lines (Shih *et al.*, 1998) will certainly

shore Taitung (Yang and Wang, 1998) shows that the top of the Luzon Arc is interpreted at a depth of 5 km with a crustal thickness of more than 20 km. According to these velocity models, the eastern boundary of the Luzon Arc offshore Taitung is about 30 km east of the coast (Yang and Wang, 1998), whereas that offshore Hualien is not clear. The eastern boundary of the northern Luzon Arc in this study may be below the eastern edge of the Hsincheng Ridge (a vertical dashed line) or extend eastward below the Hoping Basin. For the latter case, the collision of the northern Luzon Arc and the western Ryukyu Arc can be inferred.

The Ryukyu Arc basement in the lower crust cannot be identified from OBS Line 16 in this study. However, according to the velocity model of OBS Line 1 (Wang *et al.*, 1996; Wang, 1997) and the cross sections of the focal mechanisms (Kao *et al.*, 1998) in Figure 7(a), the lower crust beneath the Nanao Basin should consist of the Ryukyu Arc basement and the subducting slab of the PSP. Similarly, in view of the velocity contour and the velocity gradient in Figure 7(a), the western boundary of the PSP is inferred (an inclined dashed line) below the Hoping Basin. This westward dipping boundary may extend from 16 km to 26 km in depth along OBS Line 16. Since the PSP not only subducts northward but also appears to be westward dipping (see Figure 7(a)) owing to the northwestward motion of the PSP offshore eastern Taiwan (Seno *et al.*, 1993), part of the crust (velocity between 6 km/sec and 7 km/sec) below the Hoping Basin may move upward along the western boundary of the PSP. By considering the E-W component of the focal mechanisms in Figure 7(a), the movement of the lower crust, at least beneath the eastern portion of the Hoping Basin, may be treated as thrust faulting. The over-thrusting may further result in the eastward extension of the northern Luzon Arc and the high velocity gradient of the upper crust below the Hoping Basin, and the depression of the upper crust below the Nanao Basin. Deformation of the upper crust beneath the Hoping and the Nanao Basins described in this paper may thus be generated by the collision of the northern Luzon Arc and the western Ryukyu Arc. Other evidence of arc-arc collision has also been identified from the anomalous Poisson's ratio for the upper crust beneath the Hoping Basin (Wang *et al.*, 1998).

3.4 Moho (P-wave velocity = 7.8 km/sec)

The Moho along OBS Line 16 dips gently westward from 26 km to 33 km in depth owing to the northwestward motion of the PSP. However, the Moho below the Hoping Basin is shallower that may result from the thrusting mechanisms beneath the Hoping Basin as shown in Figure 7(a). According to Figure 5(c), the depth of the Moho is only constrained by reflections with reflection points between the Hoping Basin and the Nanao Basin (45 - 100 km from the west side of the model) while the velocity model below the Moho has no constraint. Since we cannot obtain the velocity immediately below the Moho, the Pn velocity of 7.8 km/sec in this paper is purely artificial. Further identification of the later arrivals and incorporation of other velocity models in the western Ryukyu forearc region are required to accurately determine the Pn velocity.

The constraints of the velocity model are better quantified by the normalized ray density as shown in Figure 7(b). The ray density is computed from the ray distribution and can be

promote our understanding of the Taiwan orogen and the arc-arc collision.

Acknowledgments We would like to express sincere thanks to Professor Yosio Nakamura, Dr. Kirk McIntosh and Dr. Stephane Operto for their assistance on board R/V Ocean Researcher I. We appreciate Professor Char-Shine Liu's initiation of the combined OBS and MCS survey offshore Taiwan. Professor Chi-Yue Huang and Dr. Serge Lallemand are also thanked for their preprints and suggestions about interpretations. This work has been supported by National Science Council of Taiwan under grants NSC 85-2611-M-019-003, NSC 86-2117-M019-002-ODP and NSC 87-2611-M019-011-ODP.

REFERENCES

Cheng, W. B., C. S. Wang, and C. T. Shyu, 1996: Crustal structure of the northeastern Taiwan area from seismic refraction data and its tectonic implications. *Terr. Atmo. Ocea.*, **7**, 467-487.

Chiang, C. H., 1997: Refraction survey and tectonic structures in Ryukyu forearc subduction zone offshore Hualien. Master's Thesis (in Chinese), Institute of Applied Geophysics, National Taiwan Ocean University, 88pp.

Christeson, G., 1995: OBSTOOL, software for processing UTIG OBS data. University of Texas Institute for Geophysics, Technical Report No. 134, 27pp.

Hagen, R. A., F. K. Duennebier, and V. Hsu, 1988: A seismic refraction study of the crustal structure in the active seismic zone east of Taiwan. *J. Geophys. Res.*, **93**, 4785-4796.

Henkart, P., 1998: SIOSEIS users' manual. Scripps Institution of Oceanography, University of California.

Holbrook, W. S., E. C. Reiter, G. M. Purdy, D. Sawyer, P. L. Stoffa, J. A. Austin, J. Oh, and J. Makris, 1994: Deep structure of the U.S. Atlantic continental margin, offshore South Carolina, from coincident ocean bottom and multichannel seismic data. *J. Geophys. Res.*, **99**, 9155-9178.

Hsu, S. K., and J. C. Sibuet, 1995: Is Taiwan the result of arc-continent or arc-arc collision? *Earth Planet. Sci. Lett.*, **136**, 315-324.

Hsu, S. K., J. C. Sibuet, S. Monti, C. T. Shyu, and C. S. Liu, 1996: Transition between the Okinawa Trough backarc extension and the Taiwan collision: New insights on the southernmost Ryukyu subduction zone. *Mar. Geophys. Res.*, **18**, 163-187.

Huang, C. Y., T. Byrne, C. P. Chiang, W. Y. Wu, S. J. Tsao, and T. K. Wang, 1998: Evolution of plate boundary in the Taiwan arc-continent collision terrane. *Earth Planet. Sci. Lett.*, in press.

Kao, H., S. J. Shen, and K. F. Ma, 1998: Transition from oblique subduction to collision: Earthquakes in the southernmost Ryukyu Arc-Taiwan region. *J. Geophys. Res.*, **103**, 7211-7230.

Lallemand, S. E., C. S. Liu, and Y. Font, 1997: A tear fault boundary between the Taiwan orogen and the Ryukyu subduction zone. *Tectonophysics*, **274**, 171-190.

Lallemand, S. E., C. S. Liu, S. Dominguez, P. Schnurle, J. Y. Collot, J. Y. Malavieille, and the ACT scientific crew, 1998: From oblique oceanic subduction to arc-continent col-

lision in the southern Ryukyus: New insights from detailed seafloor mapping near Taiwan, submitted to Tectonics.

Liu, C. S., D. Reed, N. Lundberg, G. F. Moore, K. D. McIntosh, Y. Nakamura, T. K. Wang, A. T. Chen, and S. Lallemand, 1995: Deep seismic imaging of the Taiwan arc-continent collision zone. *EOS, Trans. Am. geophys. Un.*, **76**, 635.

Liu, C. S., P. Schnurle, S. E. Lallemand and, D. L., Reed, 1997: TAICRUST and deep seismic imaging of western end of Ryukyu arc-trench system, In K. Fujioka ed., Deep Sea Research in Subduction Zones, Spreading Centers and Backarc Basins. *JAMSTEC J. Deep Sea Res.*, Special Vol., 39-45.

McIntosh, K. D., and Y. Nakamura, 1998: Crustal structure beneath the Nanao forearc basin from TAICRUST MCS/OBS Line 14. *TAO*, **9**, 345-362.

Operto, S., 1996: RSTTI package: Ray based seismic travel time inversion, University of Texas Institute for Geophysics. Technical Report No. 148, 40pp.

Schnurle, P., C. S. Liu, S. E. Lallemand, and D. L. Reed, 1998: Structural insight in the south Ryukyu margin: Effects of the subducting Gagua Ridge. *Tectonophysics*, in press.

Seno, T., S. Stein, and A. E. Gripp, 1993: A model for the motion of the Philippine sea plate with NUVEL-1 and geological data. *J. Geophys. Res.*, **98**, 17941-17948.

Shih, R. C., C. H. Lin, H. L. Lai, Y. H. Yeh, B. S. Huang, and H. Y. Yen, 1998: Preliminary Crustal Structures Across Central Taiwan From Modeling of the Onshore-Offshore Wide-Angle Seismic Data. *TAO*, **9**,xxxx.

Tsai, Y. B., Y. M. Hsiung, H. B. Liaw, H. P. Lueng, T. H. Yao, Y. H. Yeh, and Y. T. Yeh, 1974: A seismic refraction study of eastern Taiwan. *Petrol. Geol. Taiwan*, **11**, 165-182.

Wang, C. H., and C. H. Chen, 1988: A study of the crustal structure in the eastern Taiwan using ray tracing method, Proceedings of the Second Taiwan Symposium on Geophysics, 165-175.

Wang, T. K., K. McIntosh, Y. Nakamura, and C. S. Liu, 1996: OBS refraction survey and imaging offshore eastern Taiwan. *EOS, Trans. Am. geophys. Un.*, **77**, F720.

Wang, T. K., 1997: Shear wave structures of the crust offshore eastern Taiwan, Proceeding of Chinese Geophysical Society, 235 - 239.

Wang, T. K., S. F. Lin, W. N. Wu, C. H. Pan, and C. S. Liu, 1998: Shear and compressional wave structures explored by ocean-bottom seismometers offshore eastern Taiwan. *EOS, Trans. Am. geophys. Un.*, **79**, W74.

Yang, Y. S., and T. K. Wang, 1998: Crustal velocity variation of the western Philippine Sea Plate from TAICRUST OBS/MCS Line 23. *TAO*, **9**, 379-393.

Yeh, Y. H., R. C. Shih, C. H. Lin, C. C. Liu, H. Y. Yen, B. S. Huang, C. S. Liu, P. Z. Chen, C. S. Huang, C. J. Wu, and F. T. Wu, 1998: Onshore/Offshore Wide-Angle Deep Seismic Profiling in Taiwan. *TAO*, **9**, 301-316.

Zelt, C. A., and R. B. Smith, 1992: Seismic traveltime inversion for 2-D crustal velocity structure. *Geophys. J. Int.*, **108**, 16-34.